SAND 98-8579C

Kinematic Performance Analysis of a Parallel-Chain Hexapod Machine

Jing Song, Jong-I Mou
Arizona State University
Tempe, Arizona

Calvin King
Sandia National Laboratories
Livermore, California

Abstract

Inverse and forward kinematic models were derived to analyze the performance of a parallel-chain hexapod machine. Analytical models were constructed for both ideal and real structures. Performance assessment and enhancement algorithms were developed to determine the strut lengths for both ideal and real structures. The strut lengths determined from both cases can be used to analyze the effect of structural imperfections on machine performance. In an open-architecture control environment, strut length errors can be fed back to the controller to compensate for the displacement errors and thus improve the machine's accuracy in production.

Introduction

Traditional industrial robots are open-chain serial mechanisms constructed of consecutive links connected by rotational or prismatic joints each with one degree of freedom. They exhibit low stiffness and poor positioning accuracy, and are not suitable for large loads and high accuracy applications [1-2]. On the other hand, parallel-chain robots and machines have the advantages of (1) high force/torque capacity since the load is distributed to several in-parallel actuators, (2) high structural rigidity, and (3) better accuracy due to non cumulative joint error. Hence, in recent years increasing attention has been focused on parallel mechanisms, primarily for the improved performance they can offer in robotic and manufacturing applications [3-4].

Since proposed by Stewart in 1965 [5], parallel-chain manipulators have been used in many applications such as aircraft simulators and robot wrists. The hexapod machine is one of the recent developments based on the Stewart platform concept. Despite the aforementioned advantages over serial-chain machines and the recent technology advancement in designing and

DISCLAIMER

DISCLAIMER

Portions of this document may be illegible in electronic image products. Images are produced from the best available original document.

controlling of parallel-chain machines [6-11], the performance of parallel-chain machines is below par due to manufacturing tolerances and assembly errors. Hence, there is a need to develop a robust and effective method for hexapod machine performance assessment and enhancement.

In this paper, both inverse and forward kinematic models were derived to assess and then enhance the positioning performance of a hexapod machine located at Sandia National Laboratories, Livermore, California. A performance assessment algorithm was developed to determine the six strut lengths to drive the tool to any point within designated machine workspace. Then structural imperfections in machine component were considered in deriving another set of inverse and forward kinematic models to determine different six strut lengths that will bring the tool to the same designated location. In an open-architecture control environment, the newly determined strut length can be fed back to the controller to compensate for displacement errors due to structural imperfections and thus improve the machine's accuracy in real-time.

Inverse Kinematic Model for Ideal Structure

The configuration of the parallel-chain hexapod machine that has six identical struts is shown in Fig 1. The lower platform, called the "BASE", is a semi-regular hexagon. The upper platform, which is referred to as the "TOP", is an equilateral triangle. One end of each strut is connected to the vertices of the base platform through a three-degree of freedom universal joint. The other end of the strut is connected to another strut through a bifurcated joint first to form a pair-linked structure. Each pair-linked structure is then connected to the vertices of the top platform through a three-degree of freedom universal joints. The whole system has six degrees of freedom. The BASE frame is established by fixing the reference coordinate system (X, Y, Z) at the center of gravity of the base platform with the Z-axis pointing vertically upward. The TOP frame is established by fixing the tool coordinate system (x, y, z) at the center of gravity of the top platform with the z-axis normal to the platform and pointing outward.

Let's define the lengths of the six struts as L_1, L_2, L_3, L_4, L_5, and L_6. Denote the location of the origin of the TOP frame with respect to the BASE frame by $[P_x, P_y, P_z]$. Let (α, β, γ) represent the rotation angles defined by rotating the TOP frame first about the X-axis with α degrees, then about the Y-axis with β degrees, and finally about the z-axis with γ degree

as shown in the Figure 2. The rotation angles α and β are used to define an "approach vector" of the upper platform while γ is used to define the roll angle about the approach vector.

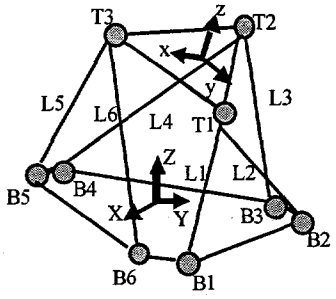

Figure 1 Hexapod Machine Configuration

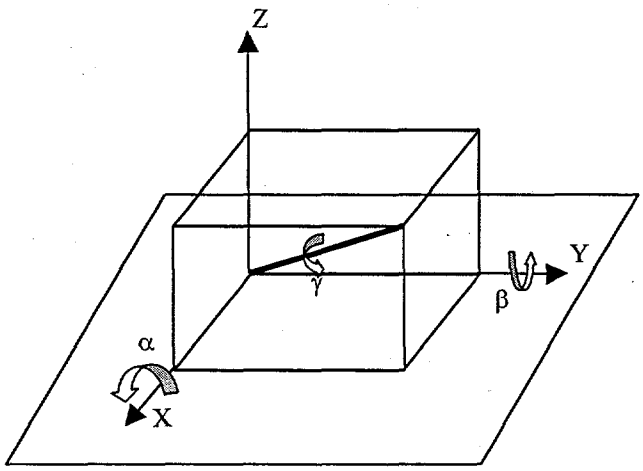

Figure 2. Rotation Angles Define Approach Vector for Top Frame

Using the Euler angle method, the transformation matrix between the mobile TOP frame and the fixed BASE frame can be derived as follows:

$$T_{BASE}^{TOP} = \begin{bmatrix} \cos\beta\cos\gamma + \sin\alpha\sin\beta\sin\gamma & -\cos\beta\sin\gamma + \sin\alpha\sin\beta\cos\gamma & \cos\alpha\sin\beta & P_x \\ \cos\alpha\sin\gamma & \cos\alpha\cos\gamma & -\sin\alpha & P_y \\ -\sin\beta\cos\gamma + \sin\alpha\cos\beta\sin\gamma & \sin\beta\sin\gamma + \sin\alpha\cos\beta\cos\gamma & \cos\alpha\cos\beta & P_z \\ 0 & 0 & 0 & 1 \end{bmatrix}$$

The coordinates of the TOP frame's vertices can be transformed to the BASE coordinate system through the transformation matrix as follows.

$$\begin{bmatrix} X_{Ti} \\ Y_{Ti} \\ Z_{Ti} \\ 1 \end{bmatrix} = T_{BASE}^{TOP}(P_x, P_y, P_z, \alpha, \beta, \gamma) \begin{bmatrix} x_{Ti} \\ y_{Ti} \\ z_{Ti} \\ 1 \end{bmatrix}$$

Thus the six struts length can then be determined as

$$L_1 = \left| \left(\vec{X}_{B_1}, \vec{Y}_{B_1}, \vec{Z}_{B_1} \right) - \left(\vec{X}_{T_1}, \vec{Y}_{T_1}, \vec{Z}_{T_1} \right) \right|$$
$$L_2 = \left| \left(\vec{X}_{B_2}, \vec{Y}_{B_2}, \vec{Z}_{B_2} \right) - \left(\vec{X}_{T_1}, \vec{Y}_{T_1}, \vec{Z}_{T_1} \right) \right|$$
$$L_3 = \left| \left(\vec{X}_{B_3}, \vec{Y}_{B_3}, \vec{Z}_{B_3} \right) - \left(\vec{X}_{T_2}, \vec{Y}_{T_2}, \vec{Z}_{T_2} \right) \right|$$
$$L_4 = \left| \left(\vec{X}_{B_4}, \vec{Y}_{B_4}, \vec{Z}_{B_4} \right) - \left(\vec{X}_{T_2}, \vec{Y}_{T_2}, \vec{Z}_{T_2} \right) \right|$$
$$L_5 = \left| \left(\vec{X}_{B_5}, \vec{Y}_{B_5}, \vec{Z}_{B_5} \right) - \left(\vec{X}_{T_3}, \vec{Y}_{T_3}, \vec{Z}_{T_3} \right) \right|$$
$$L_6 = \left| \left(\vec{X}_{B_6}, \vec{Y}_{B_6}, \vec{Z}_{B_6} \right) - \left(\vec{X}_{T_3}, \vec{Y}_{T_3}, \vec{Z}_{T_3} \right) \right|$$

Forward Kinematics Model for Ideal Structure

For a serial-link manipulator, the derivation of forward kinematic models is much simpler then that of inverse kinematics. However, for a parallel-link manipulator, the situation is reversed. A detailed report on this issue can be found in [7]. To derive the forward kinematic model, the physical dimensions of BASE and TOP structures are defined as shown in Figure 3.

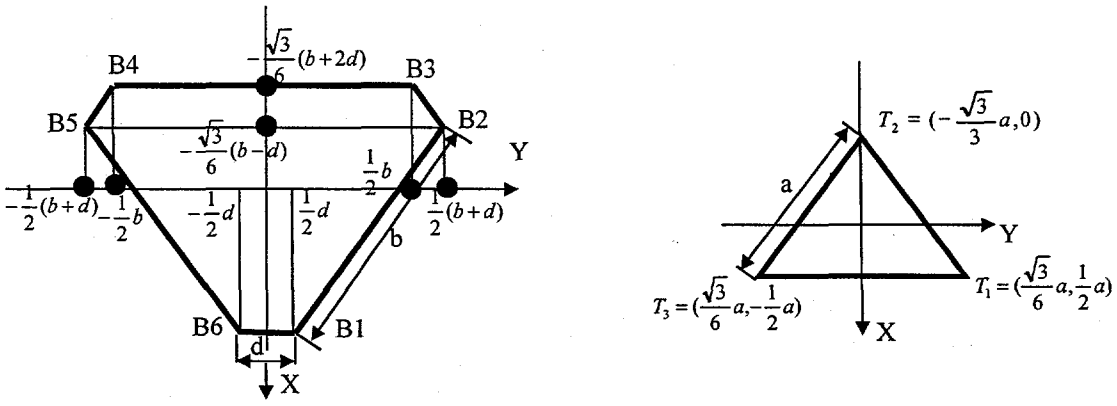

Figure 3. Physical Dimensions of Base and Top Structure

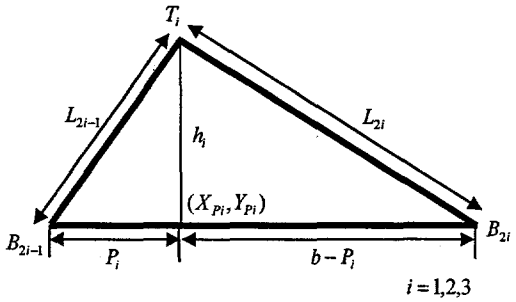

Figure 4. Geometric Relationship of Pair-Linked Structure

The kinematics transformation is the mapping from the actuator lengths L_i to the upper platform position and orientation. Once all six struts' length are determined, the geometric characteristic of all three pair-linked triangular structures ($\Delta B_{2i-1}T_iB_{2i}$; i=1,2,3) will be defined, as shown in Figure 4. The heights of the three pair-linked triangular structures (h_1, h_2, h_3) can be represented by L_i and P_i. Through simple geometric calculation, the coordinates of Xp_i and Yp_i, where i=1,2,3, can be denoted as follows.

$$p_i = \frac{1}{2b}(b^2 + L_{2i-1}^2 - L_{2i}^2); i = 1,2,3$$

$$h_i = \sqrt{L_{2i-1}^2 - p_i^2}; i = 1,2,3$$

$$X_{p1} = \frac{\sqrt{3}}{6}(2b + d - 3p_1)$$

$$Y_{p1} = \frac{1}{2}(d + p_1)$$

$$X_{p2} = -\frac{\sqrt{3}}{6}(b + 2d)$$

$$Y_{p2} = \frac{1}{2}(d - 2p_1)$$

$$X_{p3} = -\frac{\sqrt{3}}{6}(b - d - 3p_3)$$

$$Y_{p3} = -\frac{1}{2}(b + d - p_3)$$

Since the three pair-linked triangular structures ($B_1T_1B_2$, $B_3T_2B_4$, $B_5T_3B_6$) are interconnected together, they cannot move freely without constraint. Instead, the locations of T_i are limited to some certain points such that T_1, T_2, T_3 must form an equilateral triangle with fix dimensions. Although the coordinates of these TOP structure vertexes, T_i, are unknown, it is relatively easy to show that their projections on the X-Y plane can move only along the straight lines that pass through (Xp_i, Yp_I; i=1,2,3) and are perpendicular to the lower hexagonal platform, respectively. Hence, the vertexes coordinates (X_{Ti}, Y_{Ti}; i=1,2,3) of the TOP structure will be defined by the following constraints.

$$Y_{T1} = \sqrt{3}X_{T1} - (\sqrt{3}X_{p1} - Y_{p1}) = \sqrt{3}X_{T1} + \frac{1}{b}(L_1^2 - L_2^2)$$

$$Y_{T2} = Y_{p2} = \frac{1}{2b}(L_4^2 - L_3^2)$$

$$Y_{T3} = -\sqrt{3}X_{T3} - (\sqrt{3}X_{p3} - Y_{p3}) = -\sqrt{3}X_{T3} + \frac{1}{b}(L_5^2 - L_6^2)$$

The distance from vertex T_i to the intersection points (Xp_i, Yp_i; i=1,2,3) is denoted as h_i and can be calculated as follows.

$$h_i^2 = (X_{Ti} - X_{Pi})^2 + (Y_{Ti} - Y_{Pi})^2 + Z_{Ti}^2$$

To close the kinematic chain, three more constraints must be added, they are

$$(X_{T1} - X_{T2})^2 + (Y_{T1} - Y_{T2})^2 + (Z_{T1} - Z_{T2})^2 = a^2$$
$$(X_{T1} - X_{T3})^2 + (Y_{T1} - Y_{T3})^2 + (Z_{T1} - Z_{T3})^2 = a^2$$
$$(X_{T3} - X_{T2})^2 + (Y_{T3} - Y_{T2})^2 + (Z_{T3} - Z_{T2})^2 = a^2$$

By combining the above equations yields three nonlinear algebraic equations with three variables (X_{T_1}, X_{T_2}, X_{T_3}).

$$a^2 + 2X_{T1}X_{T2} - 2X_{T1}[X_{p1} + \sqrt{3}(Y_{p1} - Y_{p2})] - 2X_{p2}X_{T2} - [(\sqrt{3}X_{p1} - Y_{p1} + Y_{p2})^2 + (h_1^2 + h_2^2) - 4X_{p1}^2 - X_{p2}^2] + 2\sqrt{[h_1^2 - 4(X_{T1} - X_{p1})^2][h_2^2 - (X_{T2} - X_{p2})^2}} = 0$$

$$a^2 - 4X_{T1}X_{T3} - 2X_{T1}[X_{p1} - 3X_{p1} + \sqrt{3}(Y_{p1} - Y_{p2})] - 2X_{T3}[-3X_{p1} + X_{p3} + \sqrt{3}(Y_{p1} - Y_{p3})] - [(\sqrt{3}(X_{p1} + X_{p3}) - Y_{p1} + Y_{p3})^2 + (h_1^2 + h_3^2) - 4X_{p1}^2 - 4X_{p3}^2] + 2\sqrt{[h_1^2 - 4(X_{T1} - X_{p1})^2][h_3^2 - (X_{T3} - X_{p3})^2}} = 0$$

$$a^2 + 2X_{T2}X_{T3} - 2X_{T3}[X_{p3} + \sqrt{3}(Y_{p2} - Y_{p3})] - 2X_{p2}X_{T2} - [(\sqrt{3}X_{p3} - Y_{p2} + Y_{p3})^2 + (h_3^2 + h_2^2) - X_{p2}^2 - 4X_{p3}^2] + 2\sqrt{[h_2^2 - (X_{T2} - X_{p2})^2][h_3^2 - 4(X_{T3} - X_{p3})^2}} = 0$$

Since the derived forward kinematic models are highly nonlinear, it is impossible to solve them explicitly. Hence, for its capability of quadratic converging in the vicinity of a solution, the

Newton-Raphson numerical method is used to solve the three nonlinear algebraic equations simultaneously. Once the positions of those TOP vertexes are defined, the tool position can be determined as follows.

$$p_X = \frac{1}{3}(X_{T1} + X_{T2} + X_{T3});\ p_Y = \frac{1}{3}(Y_{T1} + Y_{T2} + Y_{T3});\ p_Z = \frac{1}{3}(Z_{T1} + Z_{T2} + Z_{T3}).$$

Inverse Kinematic Model for Real Structure

Since structural imperfections will degrade a machine's performance in producing parts, the derived kinematic models need to be modified to include the effect of those imperfections in assessing as well as enhancing the machine performance. The position errors of those ball joints located within the BASE structure can be expressed as δX_{Bi}, δY_{Bi}, and δZ_{Bi} where i=1,2,..,6. The position errors of those ball joints located within the TOP structure can be expressed as δX_{Ti}, δY_{Ti}, and δZ_{Ti} where i=1,2,3. The strut length errors can be expressed as δL_i where i=1,2,..,6. The modified inverse kinematic model for the hexapod machine can be derived from the ideal inverse kinematic model by including the error term into the original equation as follows.

$$L_1^{'} = \sqrt{(X_{T_1}^{'} - X_{B_1}^{'})^2 + (Y_{T_1}^{'} - Y_{B_1}^{'})^2 + (Z_{T_1}^{'} - Z_{B_1}^{'})^2}$$

Where

$$X_{T_1}^{'} = P_x + \left(\frac{a}{\sqrt{3}} + 2\delta X_{T_1}\right)\left[Sin\alpha Sin\beta Sin(\gamma + 60^o) + Cos\beta Cos(\gamma + 60^o)\right]$$

$$X_{B_1}^{'} = X_{B_1} + \delta X_{B_1} = \frac{\sqrt{3}}{6}(2b + d) + \delta X_{B_1}$$

$$Y_{T_1}^{'} = P_y + \left(\frac{a}{\sqrt{3}} + 2\delta Y_{T_1}\right)\left[Cos\alpha Sin(\gamma + 60^o)\right]$$

$$Y_{B_1}^{'} = Y_{B_1} + \delta Y_{B_1} = \frac{1}{2}d + \delta Y_{B_1}$$

$$Z_{T_1}^{'} = P_z + \left(\frac{a}{\sqrt{3}} + 2\delta Z_{T_1}\right)\left[Sin\alpha Cos\beta Sin(\gamma + 60^o) - Sin\beta Cos(\gamma + 60^o)\right]$$

$$Z_{B_1}^{'} = \delta Z_{B_1}$$

$$L_2^{'} = \sqrt{(X_{T_1}^{'} - X_{B_2}^{'})^2 + (Y_{T_1}^{'} - Y_{B_2}^{'})^2 + (Z_{T_1}^{'} - Z_{B_2}^{'})^2}$$

Where

$$X_{B_2}^{'} = X_{B_2} + \delta X_{B_2} = -\frac{\sqrt{3}}{6}(b-d) + \delta X_{B_2}$$

$$Y_{B_2}^{'} = Y_{B_2} + \delta Y_{B_2} = \frac{1}{2}(b+d) + \delta Y_{B_2}$$

$$Z_{B_2}^{'} = \delta Z_{B_2}$$

$$L_3^{'} = \sqrt{(X_{T_2}^{'} - X_{B_3}^{'})^2 + (Y_{T_2}^{'} - Y_{B_3}^{'})^2 + (Z_{T_2}^{'} - Z_{B_3}^{'})^2}$$

Where

$$X_{T_2}^{'} = P_x - \left(\frac{a}{\sqrt{3}} + 2\delta X_{T_2}\right)\left[Sin\alpha Sin\beta Sin\gamma + Cos\beta Cos\gamma\right]$$

$$X_{B_3}^{'} = X_{B_3} + \delta X_{B_3} = -\frac{\sqrt{3}}{6}(b+2d) - \delta X_{B_3}$$

$$Y_{T_2}^{'} = P_y - \left(\frac{a}{\sqrt{3}} + 2\delta Y_{T_2}\right)\left[Cos\alpha Sin\gamma\right]$$

$$Y_{B_3}^{'} = Y_{B_3} + \delta Y_{B_3} = \frac{1}{2}b + \delta Y_{B_3}$$

$$Z_{T_2}^{'} = P_z - \left(\frac{a}{\sqrt{3}} + 2\delta Z_{T_2}\right)\left[Sin\alpha Cos\beta Sin\gamma - Sin\beta Cos\gamma\right]$$

$$Z_{B_3}^{'} = \delta Z_{B_3}$$

$$L_4^{'} = \sqrt{(X_{T_2}^{'} - X_{B_4}^{'})^2 + (Y_{T_2}^{'} - Y_{B_4}^{'})^2 + (Z_{T_2}^{'} - Z_{B_4}^{'})^2}$$

Where

$$X_{B_4}^{'} = X_{B_4} + \delta X_{B_4} = -\frac{\sqrt{3}}{6}(b+2d) - \delta X_{B_4}$$

$$Y_{B_4}^{'} = Y_{B_4} + \delta Y_{B_4} = -\frac{1}{2}b - \delta Y_{B_4}$$

$$Z_{B_4}^{'} = \delta Z_{B_4}$$

$$L_5^{'} = \sqrt{(X_{T_2}^{'} - X_{B_5}^{'})^2 + (Y_{T_2}^{'} - Y_{B_5}^{'})^2 + (Z_{T_2}^{'} - Z_{B_5}^{'})^2}$$

Where

$$X_{T_3}^{'} = P_x + \left(\frac{a}{\sqrt{3}} + 2\delta X_{T_3}\right)\left[Sin\alpha Sin\beta Sin(\gamma - 60^o) + Cos\beta Cos(\gamma - 60^o)\right]$$

$$X_{B_5}^{'} = X_{B_5} + \delta X_{B_5} = -\frac{\sqrt{3}}{6}(b+d) - \delta X_{B_5}$$

$$Y_{T_3}^{'} = P_y + \left(\frac{a}{\sqrt{3}} + 2\delta Y_{T_3}\right)\left[Cos\alpha Sin(\gamma - 60^o)\right]$$

$$Y_{B_5}^{'} = Y_{B_5} + \delta Y_{B_5} = -\frac{1}{2}(b+d) - \delta Y_{B_5}$$

$$Z_{T_3}^{'} = P_z + \left(\frac{a}{\sqrt{3}} + 2\delta Z_{T_3}\right)\left[Sin\alpha Cos\beta Sin(\gamma - 60^o) - Sin\beta Cos(\gamma - 60^o)\right]$$

$$Z_{B_5}^{'} = \delta Z_{B_5}$$

$$L_6^{'} = \sqrt{(X_{T_2}^{'} - X_{B_6}^{'})^2 + (Y_{T_2}^{'} - Y_{B_6}^{'})^2 + (Z_{T_2}^{'} - Z_{B_6}^{'})^2}$$

Where

$$X_{B_6}^{'} = X_{B_6} + \delta X_{B_6} = \frac{\sqrt{3}}{6}(2b+d) + \delta X_{B_6}$$

$$Y_{B_6}^{'} = Y_{B_6} + \delta Y_{B_6} = -\frac{1}{2}d - \delta Y_{B_6}$$

$$Z_{B_6}^{'} = \delta Z_{B_6}$$

Forward Kinematic Model for Real Structure

The modified forward kinematic model that includes the effect of structural imperfection can be derived base on the ideal forward kinematics. Once $L_i^{'}$ (i=1, 2, ..,6) are determined, the actual tool position and orientation of the hexapod machine can then be determined as follows.

$$P_i = \frac{1}{2b_i^{'}}(b_i^{'2} + L_{2i-1}^{"\,2} - L_{2i}^{"\,2}) \qquad L_k^{"} = L_k^{'} + \delta l_k;\ k = 1,2,..,6 \qquad h_i = \sqrt{L_{2i-1}^{"\,2} - P_i^{2}};\ i = 1,2,3$$

$$b_i^{'} = \sqrt{(X_{B_{2i}}^{'} - X_{B_{2i-1}}^{'})^2 + (Y_{B_{2i}}^{'} - Y_{B_{2i-1}}^{'})^2 + (Y_{B_{2i}}^{'} - Y_{B_{2i-1}}^{'})^2};\ i = 1,2,3$$

$$X_{p_1}^{'} = \frac{\sqrt{3}}{6}(2b_1^{'} + d_1^{'} - 3p_1) \qquad X_{p_2}^{'} = -\frac{\sqrt{3}}{6}(b_2^{'} + 2d_2^{'}) \qquad X_{p_3}^{'} = -\frac{\sqrt{3}}{6}(b_3^{'} - d_3^{'} - 3p_3)$$

$$d_1^{'} = \sqrt{(X_{B_6}^{'} - X_{B_1}^{'})^2 + (Y_{B_6}^{'} - Y_{B_1}^{'})^2 + (Y_{B_6}^{'} - Y_{B_1}^{'})^2}$$

$$d_2^{'} = \sqrt{(X_{B_3}^{'} - X_{B_2}^{'})^2 + (Y_{B_3}^{'} - Y_{B_2}^{'})^2 + (Y_{B_3}^{'} - Y_{B_2}^{'})^2}$$

$$d_3^{'} = \sqrt{(X_{B_5}^{'} - X_{B_4}^{'})^2 + (Y_{B_5}^{'} - Y_{B_4}^{'})^2 + (Y_{B_5}^{'} - Y_{B_4}^{'})^2}$$

$$h_i^{'2} = (X_{T_i}^{'} - X_{P_i}^{'})^2 + (Y_{T_i}^{'} - Y_{P_i}^{'})^2 + (Z_{T_i}^{'} - (\frac{Z_{B_{2i-1}}^{'} + Z_{B_{2i}}^{'}}{2}))^2$$

$$Y_{T_1}^{'} = \sqrt{3}X_{T_1}^{'} - \frac{1}{b_1^{'}}(L_1^{"\,2} - L_2^{"\,2}) \qquad Y_{T_2}^{'} = -\frac{1}{2b_2^{'}}(L_4^{"\,2} - L_3^{"\,2}) \qquad Y_{T_3}^{'} = -\sqrt{3}X_{T_3}^{'} + \frac{1}{b_3^{'}}(L_5^{"\,2} - L_6^{"\,2})$$

$$Z_{T_1}^{'} = \sqrt{h_1^{'\,2} - 4(X_{T_1}^{'} - X_{P_1}^{'})^2} \qquad Z_{T_2}^{'} = \sqrt{h_2^{'\,2} - (X_{T_2}^{'} - X_{P_2}^{'})^2} \qquad Z_{T_3}^{'} = \sqrt{h_3^{'\,2} - 4(X_{T_3}^{'} - X_{P_3}^{'})^2}$$

By combining the derived equations, yields

$$(X_{T_2}^{'} - X_{T_3}^{'})^2 + (Y_{T_2}^{'} - Y_{T_3}^{'})^2 + (Z_{T_2}^{'} - Z_{T_3}^{'})^2 = a^2$$

$$(X_{T_i}^{'} - X_{T_3}^{'})^2 + (Y_{T_i}^{'} - Y_{T_3}^{'})^2 + (Z_{T_i}^{'} - Z_{T_3}^{'})^2 = a^2$$

$$(X_{T_i}^{'} - X_{T_2}^{'})^2 + (Y_{T_i}^{'} - Y_{T_2}^{'})^2 + (Z_{T_i}^{'} - Z_{T_2}^{'})^2 = a^2$$

The Newton-Raphson numerical algorithm is applied to solve for $X^{'}_{T_1}$, $X^{'}_{T_2}$, and $X^{'}_{T_3}$

$$P_x^{'} = \frac{1}{3}(X_{T_i}^{'} + X_{T_2}^{'} + X_{T_3}^{'}) \qquad P_y^{'} = \frac{1}{3}(Y_{T_i}^{'} + Y_{T_2}^{'} + Y_{T_3}^{'}) \qquad P_z^{'} = \frac{1}{3}(Z_{T_i}^{'} + Z_{T_2}^{'} + Z_{T_3}^{'})$$

The orientation parameter can then be determined as follows.

$$\gamma' = \arctan\left(\frac{(Y'_{T_i} - 2Y'_{T_2} + Y'_{T_3})}{\sqrt{3}(Y'_{T_i} - Y'_{T_3})}\right)$$

$$\alpha' = \arctan\left(\frac{-2[X'_{T_1}(Z'_{T_3} - Z'_{T_2}) + X'_{T_2}(Z'_{T_1} - Z'_{T_3}) + X'_{T_3}(Z'_{T_1} - Z'_{T_2})]}{a(Y'_{T_i} - 2Y'_{T_2} + Y'_{T_3})Sin\gamma + \sqrt{3}a(Y'_{T_i} - Y'_{T_3})Cos\gamma}\right)$$

$$\beta' = \arctan\left(\frac{-(Z'_{T_i} - 2Z'_{T_2} + Z'_{T_3})Cos\gamma + \sqrt{3}(Z'_{T_i} - Z'_{T_3})Sin\gamma}{(X'_{T_i} - 2X'_{T_2} + X'_{T_3})Cos\gamma - \sqrt{3}(X'_{T_i} - X'_{T_3})Sin\gamma}\right)$$

Simulation Analysis

Upon the completion of deriving the inverse and forward kinematic models that including both ideal and real structures for the hexapod machine, a simulation was implemented to test those models' robustness and reliability. The simulation program was written in C++ environment and the interface between the hexapod machine's kinematic models and the hexapod machine's open architecture controller was also implemented. So the simulation program can also be executed on the hexapod machine controller to verify its validity.

For the case of ideal structure, a set of randomly selected tool positions (x, y, z coordinates) and orientations (pitch, roll, yaw), as shown in Table 1, was first determined. Then, the inverse kinematic modeling algorithm was called to calculate the six struts' length, as shown in Table 2. Next step, the forward kinematic model was utilized, with the prior determined six struts' length as input, to estimate the tool's position and orientation, as shown in Table 3. This method was used to verify the model's consistency. The results show that the precision and consistency of the computational algorithm was about 0.01 μm.

The inverse and froward kinematic models for imperfect structure were tested with the same approach. The assumed errors include the six BASE structure joints' position error (δX_{Bi}, δY_{Bi}, δZ_{Bi}, i=1,2,…,6), three TOP structure joints' position error (δX_{Tj}, δY_{Tj}, δZ_{Tj}, j=1,2,3) and six struts' length error (δL_k, k=1,2,…,6). A random error generator was designed to produce random error value for the error terms listed above. The randomly determined values for those error terms were limited within the range of ±10 μm. Meanwhile, the error terms will have different values from iteration to iteration throughout the simulation. The purpose of this design

was to increase the inference space of the simulation in assessing the impact of structural imperfection in joints and struts on machine performance.

The same procedure for verifying the ideal kinematic models was applied to the kinematic models for real structure. The simulation results for real structure were listed in Table 4 and Table 5. The precision and consistency of the computational algorithm are about 0.1 μm.

Table 1. Simulation Input of Tool Position and Orientation
(units : mm for position & degree for orientation)

Simulation Sequence	Tool Position and Orientation					
	α	β	γ	X	Y	Z
1	0	0	0	0	0	400
2	5	0	0	0	0	400
3	0	5	0	0	5	395
4	0	0	5	5	5	405
5	5	10	5	5	0	405
6	-5	-5	0	10	5	390
7	0	0	-10	-5	-5	400
8	0	-5	5	0	-5	410
9	-5	-5	-5	5	5	390
10	5	5	5	-5	-5	390

Table 2. Simulation Result of Strut Lengths for Ideal Structure

Simulation Sequence	Strut Length (mm)					
	L1	L2	L3	L4	L5	L6
1	509.192	509.192	509.192	509.192	509.192	509.192
2	519.494	519.808	509.192	509.192	499.282	498.955
3	499.912	496.715	514.582	520.11	501.872	499.342
4	519.107	504.277	520.295	509.075	526.297	501.901
5	518.513	508.068	546.228	530.246	500.178	480.904
6	490.653	498.915	489.823	495.628	523.37	512.131
7	496.496	528.037	494.915	523.095	489.633	531.001
8	530.602	516.578	517.223	494.499	529.916	516.503
9	486.934	507.415	479.137	502.49	513.017	523.219
10	518.118	500.329	522.633	500.222	489.566	480.991

Table 3. Simulation Prediction of Tool Position and Orientation for Ideal Structure (units : mm for position & degree for orientation)

Simulation Sequence	Predicted Tool Position and Orientation					
	α	β	γ	X	Y	Z
1	7.78E-26	-6.55E-10	-3.13E-15	5.99E-09	-9.47E-15	400
2	4.99998	-6.61E-10	-2.88E-11	6.00E-09	-8.68E-11	400
3	-1.32E-11	4.99998	-5.83E-13	5.90E-09	5	395
4	-9.95E-12	-6.64E-10	4.99998	5	5	405
5	4.99998	9.99937	4.99998	5	-9.02E-11	405
6	-4.99998	-4.99998	3.57E-11	10	5	390
7	1.59E-11	-6.60E-10	-9.99938	-5	-5	400
8	3.30E-11	-4.99998	4.99998	6.05E-09	-5	410
9	-4.99998	-4.99998	-4.99998	5	5	390
10	4.99998	4.99998	4.99998	-5	-5	390

Table 4. Simulation Result of Strut Lengths for Real Structure

Simulation Sequence	Strut Length (mm)					
	L1	L2	L3	L4	L5	L6
1	509.193	509.188	509.189	509.188	509.188	509.192
2	519.494	519.804	509.19	509.19	499.279	498.955
3	499.91	496.714	514.58	520.108	501.869	499.342
4	519.105	504.274	520.293	509.071	526.294	501.899
5	518.511	508.067	546.227	530.242	500.174	480.903
6	490.653	498.913	489.822	495.626	523.365	512.129
7	496.495	528.035	494.914	523.093	489.627	531.001
8	530.601	516.579	517.22	494.496	529.914	516.503
9	486.932	507.412	479.135	502.487	513.013	523.221
10	518.118	500.327	522.632	500.218	489.564	480.991

Table 5. Simulation Prediction of Tool Position and Orientation for Real Structure (units : mm for position & degree for orientation)

Simulation Sequence	Predicted Tool Position and Orientation					
	α	β	γ	X	Y	Z
1	-7.99E-05	9.77E-06	0.000137	-0.00471	-0.00083	399.997
2	5.00001	0.00034	0.000267	-0.00378	0.000116	399.998
3	-0.00027	4.9999	-0.00035	-0.00052	4.99823	394.998
4	-0.00012	0.000232	5.00031	4.99895	4.99948	404.997
5	5.00012	9.99935	4.99992	4.99861	-0.00288	404.997
6	-4.99939	-4.99951	-8.12E-05	9.99708	4.99955	389.998
7	0.00038	0.000698	-9.99978	-5.00364	-5.00229	399.998
8	8.33E-05	-5.00067	4.99969	0.000186	-5.00182	409.998
9	-5.00048	-4.99975	-5.0003	4.99624	4.99829	389.997
10	4.9998	4.99975	5.00029	-5.00247	-5.00121	389.998

Conclusions

Inverse and forward kinematic models were derived to analyze the performance of a parallel-chain hexapod machine. Analytical models were constructed for both ideal and real structures. Performance assessment algorithm was developed to determine the six struts' lengths to drive the tool to any point within designated machine workspace with either ideal or real structures. The strut length determined from both cases can be used to analyze the effect of those structural imperfections on machine performance. In an open-architecture control environment, strut length errors can be fed back to the controller to compensate for the displacement errors and thus improve the machine's accuracy in producing parts.

Simulation results show that the derived kinematic models and corresponding computational algorithm were robust and accurate in determining the strut length for driving the tool to any location and orientation within the designated workspace. Simulation results also show that the derived inverse and froward kinematic models for real structure can be used accurately to determine a slight different strut length for driving the tool to any location and orientation within the designated workspace despite the existence of the imperfection. However, the values of those error terms due to real structure were assumed known in the simulation analysis. Nevertheless, further research need to be conducted to determine the actual joints and struts imperfections by using sensor fusion technology and mathematical inference method that are currently under investigation.

References

1. El-Khasawneh, B. S. and P. M. Ferreira, "On Using Parallel Link Manipulators as Machine Tools," *Transaction of NAMRI/SME,* Volume XXV, pp. 305-310, 1997.
2. Wang, J. and O. Masory, "On the Accuracy of a Stewart Platform - PART I, The Effect of Manufacturing Tolerances," *Proceedings of IEEE International Conference Robotics and Automation*, pp. 114-120, 1993.
3. Griffis, M. and J. Duffy, "A Forward Displacement Analysis of a Class of Stewart Platforms," *Journal of Robotic Systems*, Vol. 6, No. 6, pp. 703-720, 1989.
4. Merlet, J-P., "Direct Kinematics and Assembly Modes of Parallel Manipulators," *The International Journal of Robotics Research*, Vol. 11, No. 2, pp. 150-162, 1992.
5. D. Stewart, "A Platform with Six Degrees of Freedom," *Proc. Instn. Mech. Engrs.*, 180, No. 15, pp. 371-386, 1965.

6. Innocenti, C. and V. Parenti-Castelli, "Direct Position Analysis of the Stewart Platform Mechanism," *Mechanical Machine Theory*, Vol. 25, No. 6, pp. 611-621, 1990.
7. Liu, K., J. M. Fitzgerald, and F. L. Lewis, "Kinematic Analysis of a Stewart Platform Manipulator," *IEEE transaction on Industrial Electronics*, Vol. 40, No. 2, pp. 282-293, 1993.
8. Pang, H. and M. Shahinpoor, "Analysis of Static Equilibrium of a Parallel Manipulator," *Robotica*, Vol. 11, pp. 433-443, 1993.
9. Zhuang, H. and Z. S. Roth "Method for Kinematic Calibration of Stewart Platforms" *Journal of Robotic System*, Vol. 10, No. 3, pp. 391-405, 1993.
10. Notash, L. and R. P. Podhorodeski, "Forward Displacement Analysis and Uncertainty Configurations of Parallel manipulations with a Redundant Branch," *Journal of Robotic System*, Vol. 13, No. 9, pp. 587-60, 1996.
11. Tajbakhsh, H. and P. M. Ferreira, "Kinematic Error Estimation and Transmission Error Bounding for Stewart Platform Based Machine Tools," *Transaction of NAMRI/SME,* Volume XXV, pp. 323-328, 1997.